ACTA NEUROBIOLOGIAE EXPERIMENTALIS

Research paper Acta Neurobiol Exp 2010, 70: 423–434

Determinants of filled/empty optical illusion: search for the locus of maximal effect

Jiří Wackermann* and Kristina Kastner

Department of Empirical and Analytical Psychophysics, Institute for Frontier Areas of Psychology and Mental Health, Freiburg i. Br., Germany; *Email: jw@igpp.de

A subdivided path in the visual field usually appears longer than an empty path of the same length. This phenomenon, known as the filled/empty or Oppel–Kundt illusion, depends on multiple properties of the visual stimulus, but the functional dependences have not been yet precisely characterized. We studied the illusory effect as a function of its two main determinants, the height of vertical strokes subdividing a spatial interval of a fixed length (visual angle 2.8°) and the number of the filling strokes, using the standard–variable distance matching paradigm. Non-monotonic dependence of the effect (over-reproduction of the spatial extension) on the varied parameters was observed in two experimental series. In the first series, the maximum effect was obtained for the fillers height roughly equal to the delimiters height (visual angle 0.25°); in the second series, the maximum effect was obtained for 11–13 equispaced fillers, and more accurately estimated to 15–16 as a result of a functional fit. Both data series were successfully modeled by curves generated by a single two-parametric system of form functions. Problems of determination of the maximum effect are discussed, and arguments for a genuinely multivariate approach are presented.

Key words: beta function, geometric–optical illusions, Oppel–Kundt illusion, parametric modeling, visual space

INTRODUCTION

A path in the visual field, which is subdivided by a number of equally spaced markers, appears longer than an empty, i.e. undivided, path of the same length (Oppel 1861). This phenomenon, belonging to a large class of so-called "geometric–optical illusions" (GOI) (Oppel 1855, Helmholtz 1867, Wundt 1897, Boring 1942), is known as "illusion of interrupted extent" (Sanford 1903), "filled space illusion" (Lewis 1912), or "Oppel–Kundt illusion" (Coren and Girgus 1978, Robinson 1998, and most contemporary authors). The illusory effect is easily demonstrated in simple drawings (Fig. 1) as well as in natural life-world settings (Metzger 1975).

The Oppel–Kundt illusion (OKI) deserves a special interest for several reasons. Firstly, it is the apparent violation of additivity of perceived spatial extent, raising a fundamental problem of the proper metric of visual space. Secondly, it is its elementary character: the figure consists of an array of uniform, usually linear elements and, unlike many other GOIs, does not involve perception of angles. The figure does not provide any clues for a three-dimensional perceptual interpretation, and thus does not lend itself to popular "perspectival" explanations proposed for other kinds of GOIs (Gregory 1963, Day 1972, cf. also Robinson 1998, pp. 152ff). In contrast, the OKI invites modeling approaches seeking to explain the distortion of visual space metrics in terms of underlying physiological mechanisms (Bulatov et al. 1997, Bulatov and Bertulis 1999, Fermüller and Malm 2004, Bulatov and Bertulis 2005, Bulatov et al. 2009). Still, the OKI received less attention than other GOIs and was until recently relatively under-represented in the literature. However (thirdly), recent usage of OKI-like experimental paradigms to model the visual space anisometry observed in neurological patients (Ricci et al. 2004, Savazzi et al. 2004), and related debates (Savazzi et al. 2007, Doricchi et al. 2008), reveal not only the importance of the phenomenon, but also our limited understanding thereof.

Correspondence should be addressed to J. Wackermann
Email: jw@igpp.de

Received 20 September 2010, accepted 04 December 2010

A striking feature of the OKI is the non-monotonic dependence of the effect magnitude on the number of the subdividing elements (Knox 1894), confirmed independently by many authors (Spiegel 1937, Piaget and Osterrieth 1953, Bulatov et al. 1997): with increasing number of points or vertical lines subdividing the spatial interval, the magnitude of the illusory effect increases up to a maximum, and decreases with finer subdivision. Recently we reported that, with increasing length of the vertical lines subdividing the spatial interval, the effect is significantly reduced or vanishes completely (Wackermann and Kastner 2009). The effect thus depends non-monotonically not only on the numerosity of the interval subdivision, but also on the extent of the filling-in ("expletive") visual elements. Therefore, the term "filled/empty optical illusion" seems to be more appropriate than "illusion of interrupted extent."[1]

The aim of the present study was to examine those functional dependencies on a finer scale in order to identify more precisely the locus of maximal effect, and to model effects of both stimulus dimensions, i.e. vertical extent and numerosity of the expletive elements, by the same functional form. For this purpose, two experimental series were carried out. In Experiment 1, the number of fillers was kept constant, while their vertical extent was varied. In Experiment 2, fillers of constant height were used, while their number was varied.

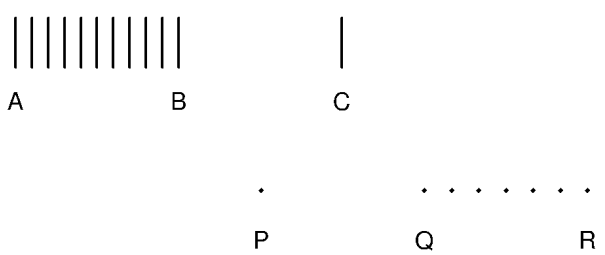

Fig. 1. Oppel–Kundt illusion. In the upper row, the distance between strokes *A* and *B* appears longer than the distance between strokes *B* and *C*, although *AB* = *BC*. In the lower row, the distance between points *Q* and *R* appears longer than the distance between points *P* and *Q*, although *PQ* = *QR*.

[1] This expression, prevailing in the Anglo-American literature, unfortunately suggests the subdivision of the interval being not just a major determining factor, but effectively the only cause of the illusion.

METHODS

Subjects

Twelve subjects, six women and six men (age range 21–33 years, mean age 24.4 years), participated in Experiment 1. Other twelve subjects, six women and six men (age range 21–32 years, mean age 24.8 years), participated in Experiment 2. Only subjects with reportedly normal vision, not using any corrective vision aids, were eligible for participation. The participants were informed about the purpose of the study, signed an informed consent before the experimental session, and received a moderate honorarium after the session. None of the participants in Exp. 1 had a previous experience with the experimental paradigm. One of the participants in Exp. 2 served in our earlier study (Wackermann and Kastner 2009), while all other subjects were naïve with respect to the experimental paradigm.

Apparatus

Stimuli were presented on a 19'' TFT monitor, connected to an iBook G4 computer, running the X11 graphics application on the Mac OS X operating system. An X11-based program *okfdisp*, specifically developed for the reported study, was used for stimulus presentation and recording of the subject's responses. Subjects were watching the display binocularly, using a chin/forehead support for the sake of comfort and to keep a constant eyes–monitor distance of 130 cms. At this watching distance and the display resolution of 1024×768 pixels, a single picture element ("pixel") was seen at angular size of exactly 1 minute of arc. The monitor was covered by a grey cardboard mask with a rectangular opening to hide the display window frame and its control elements from the subject's sight (see Wackermann and Kastner 2009, Fig. 1E). Subjects were operating with their dominant hand a pointing device ("mouse") connected via USB to the control computer, to position a movable element on the display in the experimental tasks described below.

Tasks

Two types of tasks, bisection and distance matching, were used within a single experimental session (Fig. 2a). In the bisection task, the subject was

instructed to place a movable marker V to divide a standard distance S_0S_1 into two equal halves, $S_0V = VS_1$. In the distance matching task the subject was instructed to place the marker V to reproduce the standard distance S_0S_1, so that $VS_0 = S_0S_1$. The movable element could be dragged and dropped at the destination position, or moved to the left or right with 1 pixel precision, using the wheel control of the pointing device. The final position, according to the task instruction, was confirmed by the subject's pressing simultaneously the two buttons on the pointing device. The program *okfdisp* also stored all changes of the position of the movable element V during each trial into a separate file for post hoc analyses.

The bisection task was given in the beginning of the session to make the subjects familiar with the apparatus and to practice their perception of distance equality; this was followed by the distance matching task, using different forms of the Oppel–Kundt figure (OKF) as described below. For the sake of symmetry, four variants of the distance task were used with a given stimulus type: the movable element V was placed either on the left (L) or on the right (R) side, relatively to the S_0S_1 interval, and its initial position was set either near (N) or far (F) to S_0. Each of the four variants LN, LF, RN, RF was used four times, in a pseudo-random order, with every stimulus type; consequently, there were 4 × 4 = 16 trials for every stimulus type.

Stimuli

Spatial intervals were marked/subdivided by vertical line segments of one pixel width, drawn with neutral black on a bright white background (luminosity ratio ≈1:100). The distance S_0S_1 was 336 pixels (visual angle 5.6°) in the bisection task, and 168 pixels (visual angle 2.8°) in the distance matching task. In the bisection task, and in the control condition of the distance matching task, the space between delimiters S_0 and S_1 was empty. For the distance matching task with OKF, series of stimuli were prepared with the two parameters of interest, height h and number n of the expletive elements, varied as shown in Fig. 2b, c.

Experiment 1

The space between S_0 and S_1 was subdivided by n = 20 vertical strokes into 21 equal subintervals (Fig. 2c). The height h of the strokes was varied in three series generated by the recursive formula $h_{k+1} = 2h_k + 1$. The primary series, beginning with $h_1^{(1)} = 1$, consisted of six values, 1, 3, 7, 15, 31, and 63 pixels. The secondary series, beginning with $h_1^{(2)} = 2$, consisted of five values interpolated between the elements of the primary series, namely, 2, 5, 11, 23, and 47 pixels. The tertiary series was composed of elements interpolated between neighboring elements of $h^{(1)}$ and $h^{(2)}$, that is, 4, 9, 19, 39 or 6, 13, 27, 55 pixels.

Experiment 2

The space between S_0 and S_1 was subdivided by a number n of vertical strokes of constant height, h = 15 pixels (visual angle 0.25°; Fig. 2c). The distance S_0S_1=168 pixels was chosen for the rich spectrum of its integer divisors, based on the factorization $168=2^3\times3\times7$ and resulting in fourteen stimulus types, with n varied as shown in Table I. Twelve of these fourteen stimuli were actually used in Exp. 2. Two subsets were selected from the full stimulus set, each consisting of six stimulus types: $\boldsymbol{S}_1$: n = 2, 5, 7, 13, 23 and 41, $\boldsymbol{S}_2$: n = 3, 6, 11, 20, 27 and 55. These two subsets were used alternately (each one

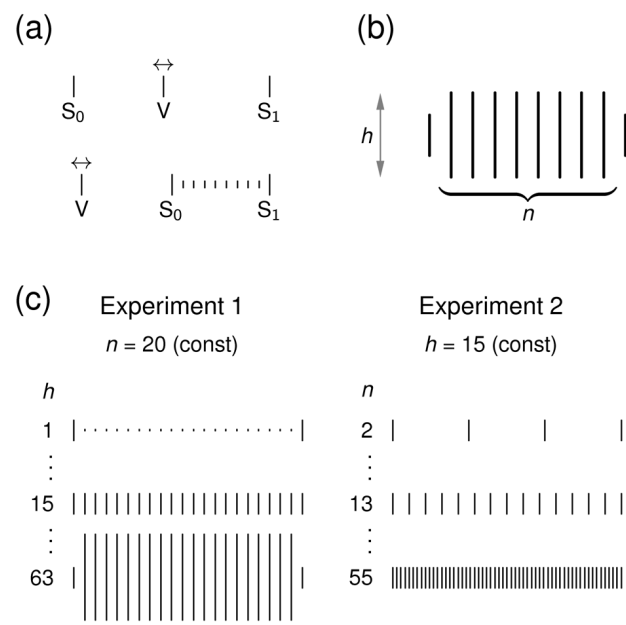

Fig. 2. Tasks and stimuli. (a) Bisection task (upper part) and distance matching task (lower part). (b) General form of the Oppel–Kundt figure (OKF) used as the stimulus in the distance matching task with n expletive elements of height h pixels. (c) Examples of OKFs with varied h or n used in Exp. 1 and 2, respectively.

Table I

Subdivisions of the spatial interval $s = S_0S_1$. Stimuli of types #2–13 were used in Experiment 2.

stimulus type #	1	2	3	4	5	6	7	8	9	10	11	12	13	14
n of dividing lines	1	2	3	5	6	7	11	13	20	23	27	41	55	83
space width $s/(n+1)$ [pixels]	84	56	42	28	24	21	14	12	8	7	6	4	3	2

with six subjects) in the main run of the experimental session.[2]

Procedures

In both Experiments 1 and 2, the experimental session started with three "warm up" trials, introducing the participant to the bisection and the distance matching task. Then the first series of 120 trials was run, beginning with 8 bisection trials and followed by 112 distance matching trials. The first 16 distance matching trials were presented with the space between S_0 and S_1 being empty (control condition). In the subsequent trials, OKFs of six different types were presented in a pseudo-random order (6×16=96 trials). The entire series thus resulted in 16+96=112 distance matching responses. Thereafter the subject's responses were sorted and average effect magnitudes (Eq. 1) were evaluated as a function of the varied parameter, i.e. the fillers height h (Exp. 1) or the number of fillers n (Exp. 2), respectively.

In Exp. 1, the main run was followed by two additional runs, each one consisting of 2 × 16 = 32 distance matching trials. In the 2nd run, two OKF types were used with filler heights h from the secondary series which were nearest to the local maximum found in the first run. In this way, a new local maximum was determined, and two adjacent values of h were chosen from the tertiary series for the 3rd run. A total of 2080 distance matching responses were collected.[3]

In Exp. 2, the main run was followed by a second run, consisting of 2 × 16 = 32 distance matching trials. A similar "bracketing" strategy was used as in Exp. 1: the two ns nearest to the local maximum were chosen from the complementary subset S_1 or S_2. A total of 1728 distance matching responses were collected.

The choice of the positioning technique, drag-and-

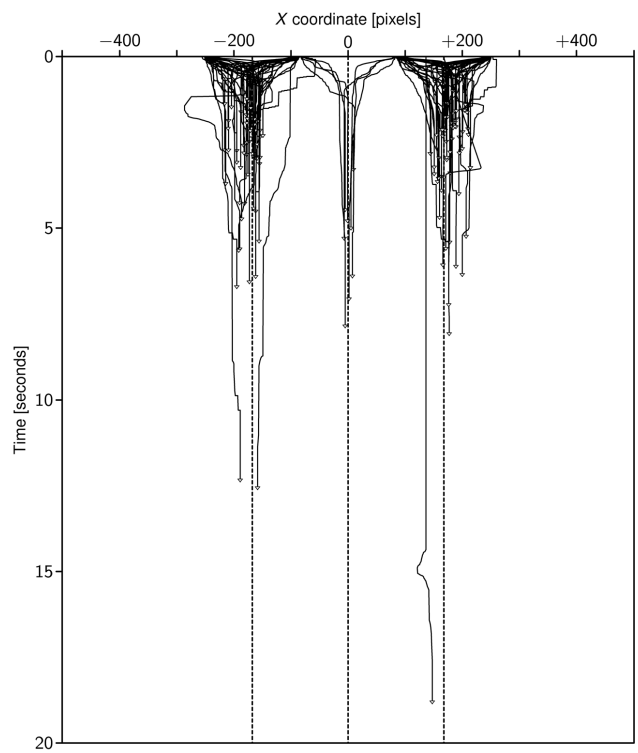

Fig. 3. Example of a single subject's motor actions from Exp. 1. Horizontal axis: position of the movable element with respect to the screen center ($X = 0$). Vertical axis: time elapsed since the beginning of the subject's response. Positioning trajectories for all 120 trials within the session are shown. The bundle of curves in the mid of the picture result from the bisection task; the left/right-hand side curve bundles result from the distance matching task with stimulus variants LN+LF and RN+RF, respectively. Open arrows mark end of each trial. The vertical dashed lines indicate geometrically correct responses for the respective tasks (bisection: $X = 0$, distance matching: $X = \pm 168$).

[2] Of the fourteen possible subdivisions listed in Table I, $n = 1$ results in the space S_0S_1 split into two halves, and $n = 83$ in a rather blurred impression of a homogeneously filled space. Since these two extreme variants qualitatively differ from perception of a uniformly subdivided but unitary space, they were omitted from the stimulus material. By division of the twelve remaining stimulus types into two complementary subsets, each consisting of six stimulus forms, the same formal design as in Exp. 1 is obtained: the control condition plus six different forms of the OKF presented in a single session.

[3] The 3rd run was omitted for one subject, who finished the 2nd run with a local maximum at $h = 3$.

drop or wheel-control, was left at the subjects' discretion. Subjects usually combined both techniques in series of stepwise approximations to the final (response) position (Fig. 3). No time limit was imposed on the participants, so that times until the response varied. The total duration of experimental sessions largely varied between subjects, typically (inter-quartile range) from 30 to 82 minutes in Exp. 1, and from 36 to 65 minutes in Exp. 2.

DATA REDUCTION AND ANALYSIS

Elimination of deviating responses

Data were first checked for responses largely deviating from the subject's central response tendency ("outliers"), which were mostly due to the subject's erroneously pressing both buttons on the response device before placing the movable element *V* at the final position. A simple "data peeling" algorithm (Appendix A) was applied, on the individual subject basis, to separate data subsets for different OKF types and variants L or R (eight trials each). The procedure was used with the same exclusion criterion ($c = 4$) on distance matching data from both experiments. This resulted in 41 outliers detected in Exp. 1 (loss rate ≈2%), and 25 outliers detected in Exp. 2 (loss rate ≈1.4%). To preserve a balanced experimental design, the outliers were replaced by arithmetic means of remaining data points for the given subject and stimulus type.

Average effects

In both experiments, the effect measure was defined as the relative deviation from the geometrically correct response,

$$r = \frac{v - s}{s}, \tag{1}$$

where $s := S_0S_1$ (standard) and $v := VS_0$ (variable). On the individual subject basis, arithmetic means of *r*s were calculated across sixteen trials available with each of the OKF stimulus types. These average effects $\overline{r}$ entered into subsequent analyses.

The literature (see Introduction) as well as the results of our previous study suggest that the expected effects are generally non-negative, i.e., zero in the control condition and positive otherwise (over-estimation of the filled spatial interval). Based on this expectation, the ratio between total sums of negative and positive effects, taken across all types of stimuli presented in the session,

$$K_{\mp} = -\frac{\sum_{\overline{r}<0}\overline{r}}{\sum_{\overline{r}>0}\overline{r}}, \tag{2}$$

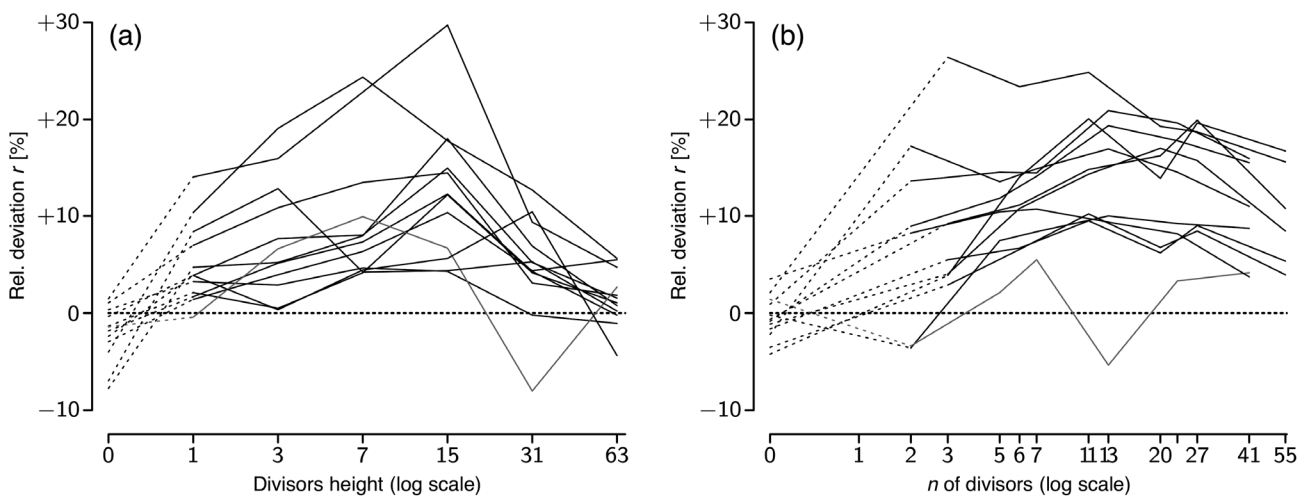

Fig. 4. Individual response curves. Displayed are individual effects (Eq. 1) $\overline{r} \times 100$ [%] as functions of the respective stimulus parameter. Exp. 1 (a): dependence on fillers height *h*; $h = 0$ indicates undivided spatial interval (control condition). Data for all 12 subjects are shown; one subject was excluded (gray curve). Exp. 2 (b): dependence on the number of fillers *n*; $n = 0$ indicates undivided spatial interval (control condition). Data for all 12 subjects are shown; one subject was excluded (gray curve).

was used as a heuristic index to detect atypical response patterns. If a subject's $K_{\mp} > 0.2$, the subject was removed from the data set.[4]

To characterize the central tendency of the response for the entire group, grand means $\overline{\overline{r}}$ were calculated from individual responses $\overline{r}$, separately for each of the stimulus types presented in the main experimental run. In Exp. 2, where stimuli from two disjunctive stimuli sets, S_1 and S_2, were used alternately, the individual response curves were first linearly interpolated for the missing values of the stimulus parameter *n*, before the grand means could be calculated. Differences of the group grand means from zero were evaluated by one-sample *t*-test.

Functional form modeling

As long as we have no theory of the OKI, which would predict the effect as a function of both variables of interest, *h* and *n*, only phenomenological data modeling is feasible. For this purpose we chose a two-parametric form function *F* which shows qualitative properties observed in the empirical response curves (Appendix B, Eq. 3). The function was matched to the grand means $\overline{\overline{r}}$ by adjusting an argument-scaling parameter *a* and a value-scaling parameter *b* to minimize the sum of squared errors (Eq. 5). In addition, the shape parameters α and β were varied interactively, beginning with $\alpha = \beta = 1$ and scanning rational values of α and β until the best possible approximation of the data was achieved.

RESULTS

Experiment 1

One subject was removed because of an atypical response curve: $K_{\mp} = 0.32$, while all other subjects had $K_{\mp} < 0.18$ (8 subjects had $K_{\mp} = 0$). The reported results are thus based on $N = 11$ subjects.

Inspection of individual response curves from the main run (Fig. 4a) reveals for most subjects (seven of eleven) an individual maximum at $h = 15$, i.e., for the fillers height *h* equal to the delimiters height h_{del}. Three subjects show maximal effect with shorter strokes, $h = 3$ or 7, while one subject has a maximum at $h = 31$. This picture is somewhat modified by the post hoc search for individual loci of maximum response in the 2nd and 3rd run: as a result, about half of the subjects (six of eleven) attained an individual maximum in the interval *h* from 15 to 19 (Fig. 5a). The values $\overline{r}$ at the points of maxima considerably vary from 5.5% to 32.8% (median 14.6%), i.e. by factor ≈6.

The group average response curve (grand means) is shown in Fig. 6a. In accord with the review of individual responses given above, the curve has a well-expressed maximum at $h = 15$, where the standard distance S_0S_1 is overestimated, on average, by 13.1%; with increasing *h* the effect turns down abruptly and practically vanishes at $h = 63$. For $1 \le h \le 31$, all grand means significantly differ from zero ($t_{df=10} > 3.17$, $P<0.01$). For $h = 0$ (empty space), the effect is marginally negative ($\overline{\overline{r}} = -0.022$, $t_{df=10} = 2.46$, $P\approx0.05$), and for $h = 63$ not significantly different from zero ($\overline{\overline{r}} = 0.014$, $t_{df=10} = 1.58$).

The form function *F* fit resulted in shape parameters $\alpha = 2/3$, $\beta = \infty$, and scaling parameters $a = 10.8$, $b = 0.118$. These parameters provide a fairly good fit (Fig. 7a) to the experimental data, except for the "overshoot" observed at $h = 15$, where the reproduced effect magnitude 11.3% is somewhat lower than the empirical value 13.1%; on the other hand, the matched function reproduces very well the rapid effect decline for $h > h_{del}$.

Experiment 2

One subject was removed because of a clearly deviant response curve: $K_{\mp} = 0.58$, while all other subjects had $K_{\mp} < 0.09$ (10 subjects had $K_{\mp} = 0$). The reported results are based on $N = 11$ subjects.

Inspection of individual response curves from the main run (Fig. 4b) reveals for six of eleven subjects

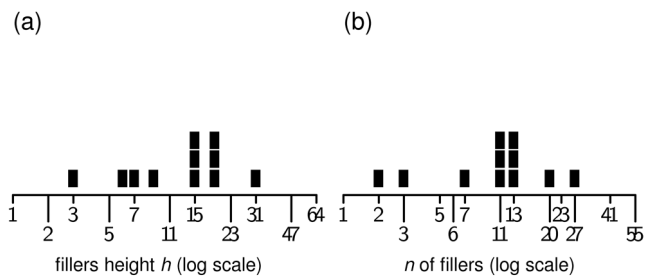

Fig. 5. Distributions of individual maximal effects. Displayed are numbers of identified loci of maximal response $\overline{r}$ as a function of (a) the fillers height *h*, varied in Exp. 1, and of (b) the number of fillers *n*, varied in Exp. 2.

[4] The critical value was set a priori, based on a simple heuristics: six different variants of the OKF figures were presented to each subject. $K_{\mp} = 0.2 = 1/(6-1)$ corresponds to the case where five positive responses are counter-acted by a negative response of the same absolute value.

maximal effects in the narrow interval $n = 11$ or 13, but maxima at extremely low values $n = 2$ or 3 were also observed, as well as a singular individual maximum at $n = 27$. The values $\bar{r}$ at the points of maxima vary from 9.5% to 26.4% (median 17.2%). This picture remains practically unchanged by the post hoc search for individual maxima (Fig. 5b).

The group average response curve (grand means) is shown in Fig. 6b. Starting with almost exactly null effect at $n = 0$ (empty space), the curve reaches a maximum at $n = 11$ and $n = 13$, where the average effect is 15.6% and 15.3%, respectively; but after a non-significant decline there is a secondary local maximum, 15.2%, at $n = 27$ (i.e., at a double filling density than the primary maximum). In sum, we observe an extended, flat region of effect saturation, instead of a well-expressed global maximum seen in Exp. 1. With n further increasing, the effect slowly decreases, dropping to ≈10% for $n = 55$. For all $n > 0$, the grand means differ significantly ($t_{df=10} > 3.17$, $P<0.01$; for $n \geq 3$ highly significantly, $t_{df=10} > 4.59$, $P<0.001$) from zero.

The form function F fit resulted in shape parameters $\alpha = 2/3$, $\beta = 3/2$, scaling parameters $a = 15.5$ and $b = 0.148$, providing an excellent fit to the data (Fig. 7b). The maximum effect is thus estimated to 14.8% at $\hat{n} = 15.5$, i.e., in the region adjacent to the empirical local maximum but not sufficiently resolved in our experimental design.

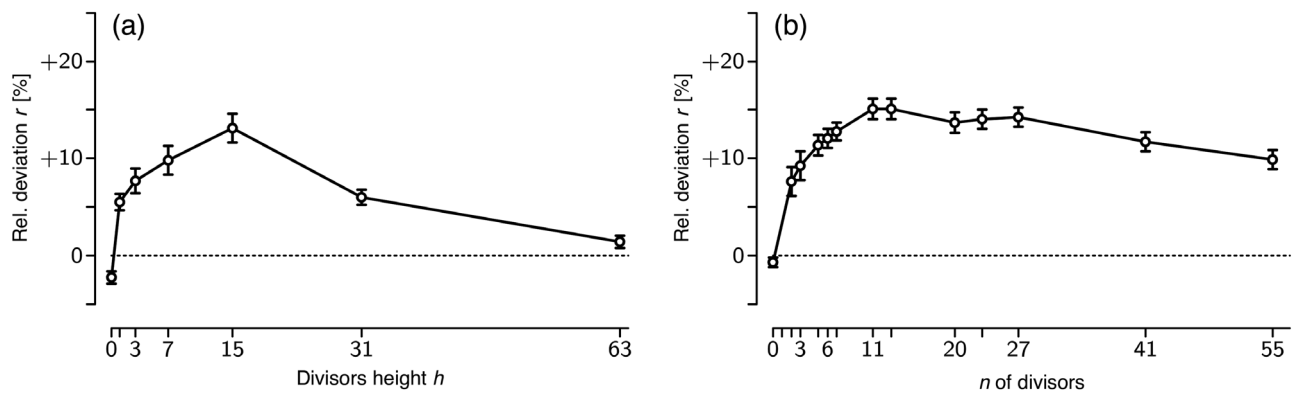

Fig. 6. Group response curves. Displayed are grand means $\bar{\bar{r}}$ (circles) ± standard errors of the means (bars) as a function of the stimulus parameter, h (Exp. 1, a) or n (Exp. 2, b), respectively. Grand means for Exp. 2 are based on individually interpolated response curves. Subjects with atypical response curves, showed in gray in Fig. 4, were excluded.

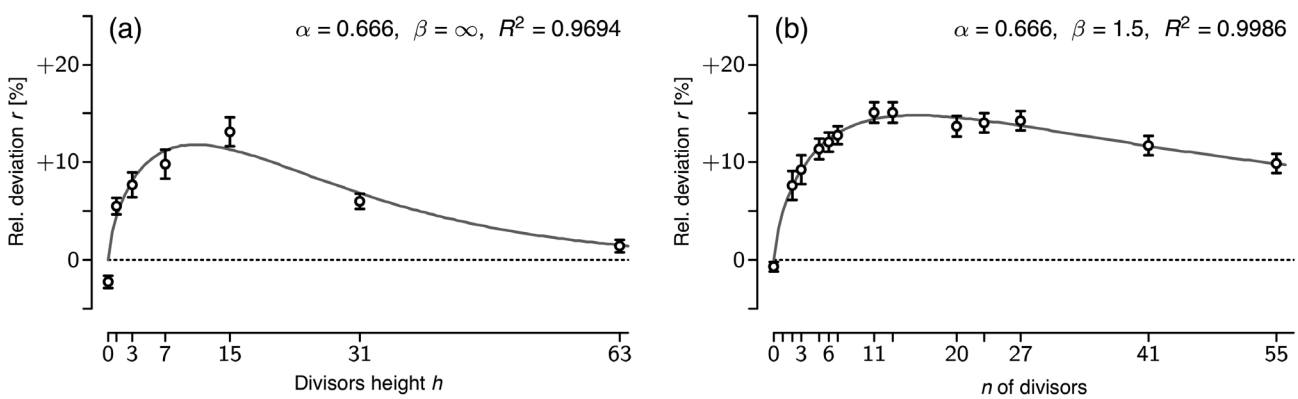

Fig. 7. Parametric fits of the form function F to group-averaged data. Displayed are grand means $\bar{\bar{r}}$ (circles) ± standard errors of the means (bars) as in Fig. 6. Exp. 1 (a): functional dependence on fillers height h for scaling parameters $a = 10.8$, $b = 0.118$, and shape parameters $\alpha = 2/3$, $\beta = \infty$ (i.e. the limiting form function G, see Eq. 4). Exp. 2 (b): functional dependence on the number of fillers n for scaling parameters $a = 15.5$, $b = 0.148$, and shape parameters $\alpha = 2/3$, $\beta = 3/2$.

DISCUSSION

The results of the presented study are generally in agreement with our previous study (Wackermann and Kastner 2009) and with the available literature; in addition, they provide a more detailed description of the OKI in terms of the two major determinants of the effect, and reveal features common to both effect dimensions.

Experiment 1

The results of Exp. 1 confirm our earlier observation: the effect measure r (relative over-estimation of the filled interval, see Eq. 1) increases with increasing height of the filling strokes h, reaches a maximum, and steeply decreases with further increasing h. The average effect magnitude at the observed maximum, 13.1%, compares well with the effect magnitude obtained in the previous study, 14.8%.

Although the present experimental design allowed to study the effect on a finer scale and within a greater dynamic range (≈5 binary orders of magnitude), the localization of the maximum remains somewhat ambiguous. In the main experimental run, the individual maxima were mostly at $h_{max} = h_{del} = 15$ arc min; the post hoc search for a more precise location shifted the h_{max} toward higher values of h (from 15 to 19); in contrast, the maximum of function F fitted to the group data is $\hat{h} = 10.8$, i.e. distinctly below h_{del}. Certainly the locus of the maximum effect is near to h_{del}, but our results do not support the categorical assertion that "equality of the lines in all respects" (Robinson 1998, p. 51) is a necessary condition for the maximal effect.

Experiment 2

The results of Exp. 2 are in qualitative agreement with earlier studies in which the number of expletive elements was systematically varied: the effect magnitude steeply increases with increasing number of the inserted elements n, reaches a relatively flat region of saturation, and slowly decreases with further increasing n. Following this typical response curve shape, most authors specified a range of maximal effect rather than a definite value: for example, Obonai (1933) found a flat maximum for n from 7 to 12 or 13 (according to Robinson 1998); Spiegel (1937) obtained maximal effects for n from 11 to 23, estimated $n = 17$ as the point of the maximum, and confirmed this estimate in post hoc experiments; Piaget and Osterrieth (1953) reported n from 9 to 14, and Bulatov et al. (1997) n from 4 to 13 as the region of maximal effect. A recent study by Bertulis et al. (2009), using modified forms of the OKF, showed a relatively well-pronounced maximum at $n = 4$. There is obviously little (if any) agreement across these reports; the search for the maximum effect seems to be hunting an elusive phantom.

Table II summarizes n_{max} (maximum observed in the data) and $\hat{n}$ (locus of maximum estimated by a function fit) from a few reports available to us, which provided sufficient information on the experimental setup and applied stimuli.[5] Disregarding differences in physical realization of the stimuli and presentation conditions, the most striking fact is the great variance of the stimulus extent in the visual field used in different studies. However, a closer inspection of the data reveals a relative invariance of the single subinterval, $s' = s / (\hat{n} + 1)$, where s = total width of the subdivided spatial interval. Except for Spiegel's data, resulting in $s' = 28.1$ arc min, other studies yield values in a quite narrow interval around ≈9 arc min: Bulatov et al. (1997): 7.9; Bertulis (2009): 9.3; our study: 10.2. Interestingly, Spiegel was the first to raise the question of the "optimal density" of the subdivision in the OKF, and proposed a linear-rational relation between n_{max} and s (Spiegel 1937, p. 338). Further experimental studies examining the important problem of scalability of the OKI are needed.

Comparison of Experiments 1 and 2

For both stimulus parameters, h and n, we observe a non-linear and non-monotonic functional dependence of the effect on the independent variable. These functional dependences can be successfully approximated by the same form function, properly scaled (Appendix B). The optimal approximations for the two experiments distinctly differ as to the shape parameter β (for vari-

[5] A comparative review of literature meets some difficulties: older sources often specify dimensions of the presented stimuli and the effect measures in length units (centimeters or millimeters), which must be recalculated to angular measures. Moreover, it has to be distinguished carefully whether the reported loci of maximal effect refer to the number of expletive elements (n in our notation), to the total number of elements composing the observed part, including the delimiters ($n+2$), or the number of resulting subintervals ($n+1$).

Table II

Locations of maximal effect observed and experimental conditions used in four different studies of the OKI.

Source reference	Maximum		Stimulus properties[a]			
	n_{max}	$\hat{n}$	width s	height h	elements	Viewing conditions
Spiegel (1937)[b]	11–23	17.0	506	64	Vert. lines, w/b	binocular
Bulatov et al. (1997)[c]	4–13	7.9	70	28	Vert. lines, b/w	monocular
Bertulis et al. (2009)[d]	4	4.4	50	2	Round dots, w/b	monocular
present study	11–13	15.5	168	15	Vert. lines, b/w	binocular

a) Visual extent of the filled spatial interval, width s × height h in minutes of arc; w/b = white figure on black background, b/w = black figure on white background.
b) n_{max} and $\hat{n}$ reported in the cited source.
c) n_{max} reported in the text, $\hat{n}$ based on data from subject #2, shown in Fig. 13 (p. 400) in the cited source.
d) n_{max} and $\hat{n}$ based on data obtained with a two-part OKF from 7 subjects, shown in Fig. 2 (p. 874) in the cited source.

able h, Exp. 1: $\beta = \infty$; for variable n, Exp. 2: $\beta = 3/2$), but yield identical values of the shape parameter $\alpha = 2/3$.[6]

Of interest is also a comparison of the response functions where the two stimulus sets, used in Exp. 1 and 2, intersect. In Exp. 2 we find for $n = 20$ average effect of 13.2%, to compare with the maximum effect magnitude of 13.1% observed in Exp. 1, where $n = 20$ was constantly used. Facing the large inter-individual variability observed in our data and considering that the two experimental series were carried out with different groups of subjects, this is an impressively good agreement, demonstrating robustness and quantitative reproducibility of the studied effect.

The synopsis of the results of Exp. 1 and 2 suggests to study the effect as a single function of the two variables, n and h. Ideally, the data-matching functions found in univariate experiments should result from a general functional model as special cases. As seen above, already simple univariate designs result in time-consuming experimental series, so that full factorial experimental designs are not practicable. If more advanced methods such as response surface modeling (e.g. Khuri 2006) are to be used, an adequately parameterized multivariate model—in other words, a "phenomenological theory" (Wackermann 2010)—of the effect is desirable.

6 Whether this identity is merely a matter of coincidence, or reveals some deeper invariance underlying the oki effect, is an open question for further studies.

General remarks and outlook

This reasoning leads to the problem of a sufficient (even if not exhaustive) characterization of the effect under study: what is the minimal set of stimulus parameters to enter such a phenomenological theory? Whereas early explanatory attempts (Hering 1861, Kundt 1863, Wundt 1897) considered the number of subdividing elements n as the only relevant variable, with later studies varying the appearance of the expletive elements (e.g. Spiegel 1937, Bulatov and Bertulis 2005, Wackermann and Kastner 2009), their spacing (e.g. Lewis 1912, Piaget and Osterrieth 1953), or their visual contrast (Dworkin and Bross 1998), the number of significant stimulus dimensions gradually increased. An elaborated theory of the phenomenon will have to account not only for the univariate effects, but also for their interplay if two or more stimulus parameters are varied. In a multivariate approach, the maximum effect locus is not just a point on a selected dimension (a number), but generally a multidimensional manifold in the space of stimulus parameters. The form of the locus may provide a qualitative signature of the effect, against which models and theories could be tested.

CONCLUSION

The reported study aimed at the quantitative characterization of the Oppel–Kundt phenomenon as a function of two major determinants, namely, extension and numerosity of the expletive elements (fillers).

1. The non-monotonic dependence of the effect on the vertical extent of the expletive elements, observed in our earlier study, was confirmed. The effect reaches a maximum for the filling strokes of approximately same height as that of the delimiters (here: 15 arc minutes) and rapidly declines to zero with further increasing height.

2. The non-monotonic dependence of the effect on the number of the expletive elements, reported in several preceding studies, was confirmed. The effect reaches a maximum for 15–16 filling strokes and declines only slowly with further increasing numerosity of the interval subdivision. The flat shape of the response curve in the region of the maximal effect, and inter-subject variability of individual responses, account for reported difficulties in the determination of the maximum.

3. The effect magnitude was modeled separately as a function of the two stimulus variables, fillers height h and number of filling elements n. Fairly good to excellent fits were obtained with functional forms from a two-parametric system of functions, resulting in a more accurate determination of the loci of maximal effect, and suggesting a possibly unifying mathematical expression of the effect as a multivariate function of relevant stimulus properties.

4. The large variance between reports from different studies suggests that the specification of the effect maximum by the number of the expletive elements may be inadequate, and some other characteristic invariants of the effect should be searched for. The angular extent of a single subinterval of the Oppel–Kundt figure is suggested as a possible candidate.

5. A genuinely multivariate approach to the studied phenomenon, aiming at characterization of the effect in the multidimensional space of stimulus parameters, is recommended,

ACKNOWLEDGEMENT

We thank Werner Ehm, Marc Wittmann, and two anonymous reviewers for critical comments on earlier versions of the manuscript, Aleksandr Bulatov and Hans-Georg Geißler for helpful discussions, and Oksana Gutina for organizational and technical assistance. Finally, we wish to thank all participants for their time and patience.

APPENDIX

A. Elimination of deviating responses

Given a data sample $x_1,\ldots, x_n$, a measure of deviation of the element x_j from the residual sample is defined as

$$z_j = \frac{x_j - m}{\sqrt{v}}$$

where

$$m = \frac{1}{n-1}\sum_{i\neq j} x_i \ , \ v = \frac{1}{n-2}\sum_{i\neq j}(x_i - m)^2 \ ,$$

are arithmetic mean and variance of the residual sample, respectively. If $|z_j| > c$ (an a priori chosen constant), the element x_j is marked as 'outlier' and removed from the sample; the procedure is then applied iteratively until there are no more outliers detected. A reasonably conservative exclusion criterion, $c = 4$, was used throughout the data analyses.

B. Definition and properties of the form function

For the purpose of mathematical modeling of response curves we chose a function

$$F(x) = x^{\alpha}\left(\frac{\alpha + \beta}{\alpha\, x + \beta}\right)^{\alpha+\beta} \qquad (x \geq 0), \tag{3}$$

with two adjustable parameters $\alpha, \beta > 0$, allowing for fine tuning of the function's shape. Function F shows qualitative features observed in the empirical response curves:

(i) no effect in the control (baseline) condition: $F(0) = 0$;

(ii) asymptotic decline of the effect with increasing stimulus variable: $\lim_{x\to\infty} F(x) = 0$;

(iii) existence of a unique maximum, fixed at $F(1) = 1$.

Function F has been obtained from function $t^{\alpha}(1-t)^{\beta}$ [which is known from the theory of beta function (Abramowitz and Stegun 1965) and has wide applications in mathematical statistics] by substitution $x/(x+c) \to t$. Putting $c = \beta / \alpha$, the composed function has a maximum at $x = 1$; normalizing to $F(1) = 1$ yields

the function form given by Eq. (3). The limiting form of function F for $\beta \to \infty$ is

$$G(x) = x^{\alpha} e^{-\alpha(x-1)}, \quad (4)$$

shape of which is determined by only one parameter, α. Eq. (4) can be obtained directly from the density function of the gamma distribution by fixing its maximum at $x = 1$ and normalizing to $G(1) = 1$.

Given the form function F, a response curve $r = (r_j)$ is modeled by $b\,f = (b\,f_j)$, where $f_j := F(x_j/a)$ are values of the scaled form function at sampling points x_j ($j = 0, \ldots, l$) of the stimulus parameter varied in the experiment (h or n). The scaling parameters a, b are adjusted to minimize the error criterion

$E = \| r - b\,f \|^2$.

For a fixed value of a, E attains minimum for,

$$b = \frac{\boldsymbol{f} \cdot \boldsymbol{r}}{\| \boldsymbol{f} \|^2} \quad (5)$$

which gives

$$E = \| \boldsymbol{r} \|^2 \left(1 - \frac{(\boldsymbol{f} \cdot \boldsymbol{r})^2}{\| \boldsymbol{f} \|^2 \| \boldsymbol{r} \|^2} \right) = \| \boldsymbol{r} \|^2 \left(1 - R^2 \right).$$

The global minimum of E is found by a simple comparative interval-split method, with a varied in a predefined range; the term R^2 provides a goodness-of-fit measure.

REFERENCES

Abramowitz M, Stegun IA (1965) Handbook of mathematical functions. Dover, New York.

Boring EG (1942) Sensation and perception in the history of experimental psychology. Appleton–Century–Crofts, New York.

Bertulis A, Surkys T, Bulatov A, Gutauskas A (2009) Three-part Oppel–Kundt illusory figure. Medicina (Kaunas) 45: 871–877.

Bulatov A, Bertulis A, Mickienė L (1997) Geometrical illusions: study and modelling. Biol Cybern 77: 395–406.

Bulatov A, Bertulis A (1999) Distortions of length perception. Biol Cybern 90: 185–193.

Bulatov A, Bertulis A (2005) Distracting effects in length matching. Acta Neurobiol Exp (Warsaw) 65: 265–269.

Bulatov A, Bertulis A, Bulatova N, Loginovich Y (2009) Centroid extraction and illusions of extent with different contextual flanks. Acta Neurobiol Exp (Wars) 69: 504–525.

Coren S, Girgus JS (1978) Seeing is deceiving: the psychology of visual illusions. Lawrence Erlbaum, Hillsdale (NJ)

Day RH (1972) Visual spatial illusions: a general explanation. Science 175: 1335–1340.

Dworkin L, Bross M (1998) Brightness contrast and exposure time effects on the Oppel–Kundt illusion. Perception 27: ECVP Abstract Suppl.

Doricchi F, Guariglia P, Figliozzi F, Silvetti M, Gasparini M, et al. (2008) No reversal of the Oppel–Kundt illusion with short stimuli: confutation of the space anisometry interpretation of neglect and 'cross-over'in line bisection. Brain 131: 1–4.

Fermüller C, Malm H (2004) Uncertainty in visual processes predicts geometrical optical illusions. Vision Res 44: 727–749.

Gregory RL (1963) Distortion of visual space as inappropriate constancy scaling. Nature 199: 678–680.

Helmholtz H (1867) Handbuch der physiologischen Optik, Vol. 3. Barth, Leipzig.

Hering E (1861) Beiträge zur Physiologie, Vol. 1. Engelmann, Leipzig.

Khuri AI, ed. (2006) Response surface methodology and related topics. World Scientific, Singapore.

Knox HW (1894) On the quantitative determinants of an optical illusion. Am J Psychol 6: 413–421.

Kundt A (1863) Untersuchungen über Augenmaass und optische Täuschungen. Ann Phys Chem 196: 118–158.

Lewis EO (1912) The illusion of filled space. Brit J Psychol 5: 36–50.

Metzger W (1975) Gesetze des Sehens, 3rd ed. Kramer, Frankurt.

Obonai T (1933) Contributions to the study of psychophysical induction: III. Experiments on the illusions of filled space. Jap J Psychol 8: 699–720.

Oppel JJ (1855) Ueber geometrisch-optische Täuschungen. Jahresber phys Verein Frankfurt 1854/1855: 37–47.

Oppel JJ (1861) Ueber geometrisch-optische Täuschungen (Zweite Nachlese). Jahresber phys Verein Frankfurt 1860/1861: 26–37.

Piaget J, Osterrieth PA (1953) Recherches sur le développement des perceptions: XVII. L'évolution de l'illusion d'Oppel–Kundt en fonction de l'âge. Arch de Psychol, 34: 1–38.

Ricci R, Pia L, Gindri P (2004) Effects of illusory spatial anisometry in unilateral neglect. Exp Brain Res 154: 226–237.

Robinson JO (1998) The psychology of visual illusion, 2nd ed. Dover, Mineola (NY).

Sanford EC (1903) A course in experimental psychology. Heath, Boston.

Savazzi S, Frigo C, Minuto D (2004) Anisometry of space representation in neglect dyslexia. Cogn Brain Res 19: 209–218.

Savazzi S, Posteraro L, Veronesi G, Mancini F (2007) Rightward and leftward bisection biases in spatial neglect: two sides of the same coin? Brain 130: 2070–2084.

Spiegel HG (1937) Über den Einfluß des Zwischenfeldes auf gesehene Abstände. Psychol Forsch 21: 327–383.

Wackermann J (2010) Geometric–optical illusions: a pedestrian's view of the phenomenal landscape. In: Bastianelli A, Vidotto G (eds.), Fechner Day 2010. International Society for Psychophysics, Padova. pp. 171–176.

Wackermann J, Kastner K (2009) Paradoxical form of filled/empty optical illusion. Acta Neurobiol Exp (Wars) 69: 560–563.

Wundt W (1897) Die geometrisch-optischen Täuschungen. Abh Königl Sächs Gesellsch Wiss 42: 55–178.